J. Shimwell, L. Morgan, S. Lilley, M. Kovari, S. Zheng, J. McMillan

Spatially and temporally varying transmutation in solid-type breeder blankets

Spatially and temporally varying transmutation in solid-type breeder blankets

J. Shimwell[a], L. Morgan[b], S. Lilley[b], M. Kovari[b], S. Zheng[b], J. McMillan[a]

[a]*Department of Physics and Astronomy, University of Sheffield, Hicks Building, Hounsfield Road, Sheffield, S3 7RH, UK.*
[b]*Culham Centre for Fusion Energy, Culham Science Centre , Abingdon, Oxfordshire , OX14 3DB, UK.*

Spatially and temporally varying transmutation in solid-type breeder blankets.

J. Shimwell[a,*], L. Morgan[b], S. Lilley[b], M. Kovari[b], S. Zheng[b], J. McMillan[a]

[a]*Department of Physics and Astronomy, University of Sheffield, Hicks Building, Hounsfield Road, Sheffield, S3 7RH, UK.*
[b]*Culham Centre for Fusion Energy, Culham Science Centre , Abingdon, Oxfordshire , OX14 3DB, UK.*

Abstract

High energy neutrons produced in future fusion reactors will cause significant transmutation reactions in the breeder blanket, including the important tritium breeding reactions. The reaction rate for a given reaction type depends on the neutron spectrum and material properties. The inventory consequences for tritium production of a solid-type breeder blanket are discussed in this paper. A DEMO fusion reactor with 19 homogeneous breeder blanket modules made of Eurofer, helium, $Be_{12}Ti$ and Li_4SiO_4, with enriched ^6Li content. Each blanket module was segmented radially in order to analyse the time-dependent reaction rate as a function of depth. The resolution of radial segmentation was varied and 5 radial divisions were found to be sufficient to accurately model the tritium inventory. Time-dependent tritium production was simulated with the use of the interface code, FATI, which couples radiation transport code MCNP 6 with the inventory code FISPACT-II. The simulated results show how the tritium production varies over the expected lifetime of the blanket. The overall tritium production of the solid-type blanket decreases as the ^6Li and ^7Li are burnt up. The effect of ^6Li burn-up in the breeder zones nearest to the plasma is identified as the main contributing factor to the decreasing tritium production of the whole breeder blanket.

Keywords: Fusion, tritium, inventory, neutronics, burn-up, blanket.

1. Introduction

Fusion energy has the potential to provide a sustainable source of energy, which will help address the global energy need. The most achievable fusion reaction requires deuterium (D), which is available from seawater and tritium (T) available through Li reactions. However, there is currently no sustainable source of T to allow for long term operation of a fusion reactor. A sufficient amount of T could be produced in heavy water reactors to provide a limited start up inventory. One of the critical roles of a DEMOnstration fusion power plant (DEMO) will be to establish breeder blanket technology that is capable of meeting the T demands of fuelling the (D-T) plasma. Blanket designs capable of breeding T will be trialled in ITER. Blankets such as the Helium Cooled Pebble Bed (HCPB) [1] have undergone neutronic design optimisation [2, 3] to ensure T self-sufficiency. This is particularly challenging when considering the burn-up of ^6Li, ^7Li and ^9Be.
Aside from ensuring T self-sufficiency predictions of the surplus T inventory are of interest for subsequent fusion power plants requiring a start-up inventory. Predicting the maximum T storage requirements will be necessary for safety licensing. Here we present simulations of the tritium breeding ratio (TBR) and T inventory over the expected life-time of the breeder blanket. The research builds on the work of [4, 5, 6, 7]. In our simulation we use a DEMO 3D geometry containing homogenised breeder blankets that are segmented both radially and toroidally to examine the effects of spatial resolution of the breeder blanket on the T inventory. The computational advantages of homogenised models over more detailed heterogeneous models make them attractive for burn-up and parametric studies.

2. Material and methods

The reactor model was adapted from a tokamak DEMO model developed byt KIT under an EFDA 3PT task [8]. The model includes first wall, homogenised breeder modules and a rear shielding layer. The breeder zones were split toroidally into 19 modules and up to 10 segments radially (see Figure 6). The neutron source geometry was based on the plasma parameters: 9 m major radius; 2.25 m minor radius; triangularity of 0.33;

---
*Corresponding author
Email address: mail@jshimwell.com (J. Shimwell)

peaking factor of 1.3; and an elongation of 1.66. The 14.1 MeV neutron source used birth locations based on the plasma density and temperature and emitted isotropically. The magnets were defined as Nb_3Sn and the vacuum vessel from 316 stainless steel. A 3 mm layer of pure tungsten was defined as the plasma facing component (the first wall) [9]. The reduced activation steel Eurofer [10] with a helium coolant (3cm thick and homogenised) was selected as the material for the front and rear casing of the breeder blankets. Details of the materials used in the breeder zone can be found in Table 1. Eurofer was used as a structural material within the breeder blankets. Helium is both the coolant and purge gas. $Be_{12}Ti$ was selected as the neutron multiplier instead of beryllium metal due to its performance capability at higher temperatures [11]. Li_4SiO_4 with a ^6Li enrichment of 40% was selected as the ceramic breeder material. Both the $Be_{12}Ti$ and the Li_4SiO_4 were assumed to be in pellet form with a packing fraction of 0.63. The thickness of the inboard blankets was 0.75 m and the outboard blankets was 1.30 m. A Monte

Material	Component	Volume percent	Resultant density (g/cm^3)
Homogenized breeder material	Eurofer	9.705	1.816
	He coolant	5.295	
	Li_4SiO_4	9.450	
	He purge gas	31.45	
	$Be_{12}Ti$	44.10	

Table 1: Material specifications for the homogeneous breeder blanket material.

Carlo approach utilising MCNP 6 [12] was used to simulate neutron transport. The inventory code FISPACT-II [13] was used to model activation, transmutation and neutron-induced burn-up. The interface code FATI [14] was used which couples MCNP 6 and FISPACT-II together. FENDL 3.0 [15] nuclear data was used preferentially for particle transport. TENDL 2014 [16] nuclear data was used by FISPACT-II to model activation, transmutation, neutron-induced burn-up and also for particle transport when FENDL data was not available. Recent investigations into the effect of different sized time steps have be carried out [17] and time steps of less than one month were recommended. Burn-up was simulated in time steps of 15 days for a fusion reactor with 2.4GW of fusion power, operating 70% [18] of the time. The T inventory is the difference between production of T in the blanket and consumption in the plasma, accounting for T decay. Leakage, retention and isotope separation

efficiencies of T were not accounted for in this simulation. H and He isotopes produced within the burn cells during irradiation were assumed to be removed from the breeder zones in the purge gas flow.

3. Theory

Tritium is produced within a fusion breeder blanket, predominantly via the $^6Li(n,t)$ reaction; the $^7Li(n,n't)$ reaction also contributes via higher energy neutrons. Another key threshold reaction is $^9Be(n,2n)$ which serves to increase the neutron flux. As the material is transmuted the changing composition will result in a time-varying reaction rate, which results in a time-varying neutron spectrum. The neutron spectrum also varies spatially within the tokamak.

The rate of T production depends upon the neutron spectrum and regions which experience significantly different spectra should be modelled separately. Modelling regions with significantly different neutron spectra collectively causes a smearing effect as material transmutations occurring predominantly at one location are averaged across the cell. The majority of lithium depletion occurs at the region of the breeder blanket nearest to the plasma due to the high neutron flux. The spatial resolution of the MCNP model must be sufficiently high to account for localised burn-up within the blanket, otherwise the simulation would effectively be replenishing lithium supplies at the inner surface of the breeder blanket and overestimate T production. Figure 1 shows how the neutron spectrum and, in particular, the 14.1 MeV component vary with blanket depth. The blanket
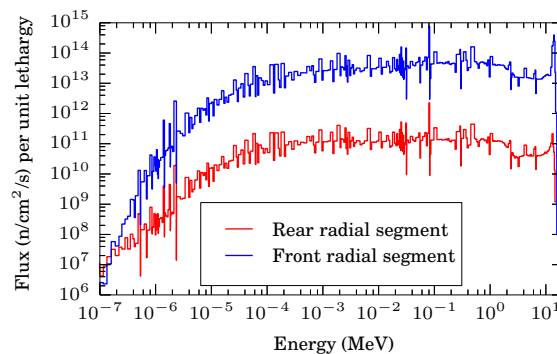

Figure 1: Neutron spectra for different locations in the equatorial outboard blanket module at the first time step.

modules also receive different neutron fluxes (see Figure 2), this is largely due to the varying proximity of the breeder modules to the neutron source and the distribution of neutrons within the source geometry. As materials are irradiated transmutation and decay processes
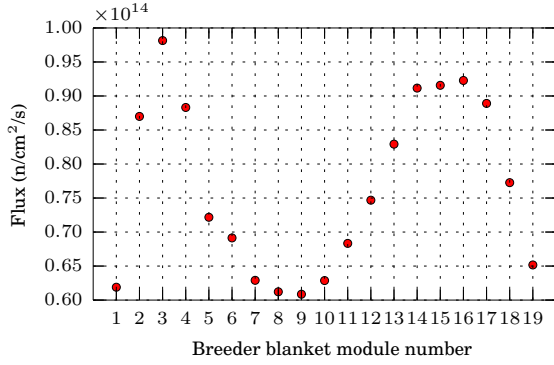
Figure 2: Neutron flux incidence on the first wall of each breeder module. See Figure 6 for module numbers.

change the material composition, affecting the neuronic behaviour. The consequence of the changing material composition is a time-varying spectra (see Figure 3). Nuclei with large capture cross sections are burnt-up more rapidly and therefore slight increases in the flux at lower energies is observable over long irradiation periods.
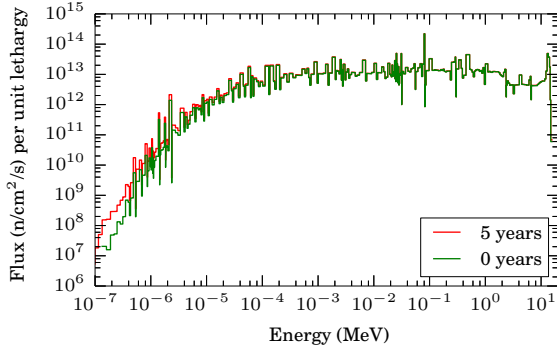

Figure 3: Neutron spectra at two irradiation times for the equatorial outboard blanket module.

4. Results

We have investigated spatial segmentation of breeder blankets. Ideally the mean free path of a neutron within the material would determine the segmentation size, however such accuracy is computationally expensive. FATI simulations were performed for the DEMO models allowing the TBR and T inventory as a function of radial segments to be investigated. The TBR of the system decreases as a function of time, but remains above 1, as shown in Figure 4, which also shows the T inventory. The TBR and T inventory of the breeder blanket with only 1 segment remained higher than the more finely segmented models for the five year irradiation time. The TBR and T inventory for models

with 5 or more radial segments converge to the same value. The increased geometrical complexity and computational time for segmenting the model beyond 5 segments only fractionally increased the accuracy of the TBR and T inventory prediction (see Figure 5). Figure
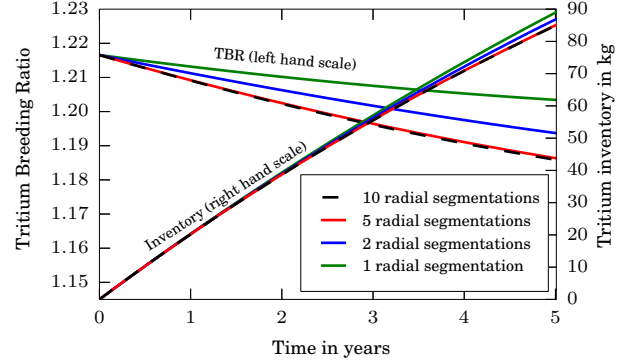

Figure 4: TBR (fitted) and the associated T inventory. Only simulations with 1, 2, 5 and 10 segmentations are shown for clarity. Error bars were derived from MCNP tally uncertainties and represent a 1 sigma confidence.

5 suggests that modelling this particular breeder blanket as a single homogeneous segment overestimates the T inventory at five years by 4kg.
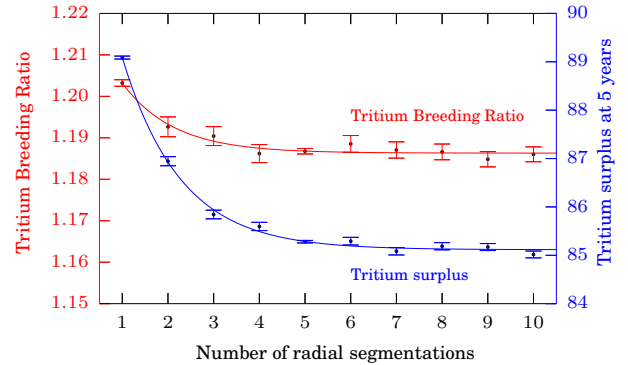

Figure 5: TBR and T inventory after five years for differently segmented blanket models. Error bars were derived from MCNP tally uncertainties and represent a 1 sigma confidence.

^{6}Li burn-up is not uniform throughout the blanket due to the different spectrum experienced at different locations. Figure 6 shows the percentage of the original ^{6}Li remaining after 5 years. The ^{6}Li depletion is highest (81% remaining) at the inner segment of blanket module 3. Whereas, the ^{6}Li burn-up in the outer segment of blanket module 19 is negligible (0.1%). The modules are divided into segments with equal percentages of the overall module thickness and therefore the ^{6}Li depletion is averaged over cells of different thicknesses.
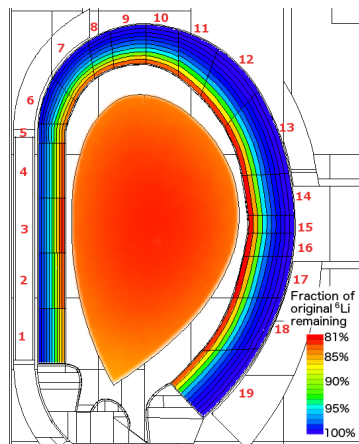
Figure 6: ^{6}Li depletion throughout the breeder blanket after 5 years and neutron source intensity. Breeder blanket modules are numbered.

5. Discussion

We find that calculated TBR declines more rapidly due to burn-up of lithium when blanket modules are radially segmented in the model. These results imply that some previous studies of T inventories in homogenised breeder blanket models may have overestimated T production over time due to lack of radial segmentation. Although 5 radial segmentations appears to be sufficient for this particular model, heterogeneous breeder blanket models are likely to require finer segmentation. This is because the lithium ceramic regions are often separated by structural materials or cooling components and the spectra is likely to be different on either side of these components.

By performing these simulations we see that ^{6}Li burn-up varies throughout the blanket and some regions are under utilised while other areas experience high ^{6}Li burn-up. Tailoring the blanket composition to suit the incident neutron spectra could improve the durability of the blanket while potentially reducing the material cost. This could be achieved by varying the ratio of neutron multiplier to lithium ceramic or the ^{6}Li enrichment.

6. Conclusion

TBR simulations have been carried out for breeder blankets with toroidal and radial segmentation. From this research the following conclusions are made.

- A fine spatial resolution has been shown to be necessary for accurate predictions of the T inventory when simulating time-dependent TBR in homogenised solid-type breeder blankets.
- Five radial segmentations were found to be sufficient when ^{6}Li burn-up is not more than 20%.
- Segmentation of the blanket cells allows the simulation to take account of the variation neutron spectrum through the blanket.

While cell based division is able to provide the required spatial resolution for this model it may be less suitable for heterogeneous breeder blankets. The shape of regions experiencing similar spectra is likely to be more complex for detailed breeder blanket designs. A mesh based approach to burn-up could be advantageous to facilitate more optimal geometric divisions.

7. Acknowledgments

8. References

[1] L.V Boccaccini et al. Materials and design of the european DEMO blankets. *J. Nucl. Mater.*, 329-333:148–155, 2004.

[2] U. Fischer et al. Neutronic design optimisation of modular HCPB blankets for fusion power reactors. *Fusion Eng Des*, 75-79:751–757, 2005.

[3] P. Pereslavtsev et al. Neutronic analysis of the HCPB TBM in ITER utilizing an advanced integral approach. *Fusion Eng Des*, 85:1653–1658, 2010.

[4] A. Aures et al. Tritium self-sufficiency of HCPB blanket modules for DEMO considering time-varying neutron flux spectra and material compositions. *Fusion Eng Des*, 88, 2013.

[5] S. Sato et al. Effects of lithium burn-up on TBR in DEMO reactor slimcs. *Fusion Eng Des*, 87:680–683, 2012.

[6] B.R. Colling et al. Development of fusion blanket technology for the DEMO reactor. *Appl. Radiat. Isot.*, 70:1370–1372, 2012.

[7] L.W. Packer et al. Tritium self-sufficiency time and inventory evolution for solid-type breeding blanket materials for DEMO. *J. Nucl. Mater.*, 417:718–722, 2011.

[8] P. Pereslavtsev et al. Generation of the mcnp model that serves as a common basis for the integration of the different blanket concepts. *EFDA D 2M7GA5 V.1.0*, 2013.

[9] Y. Igitkhanov et al. Applicability of tungsten EUROFER blanket module for the DEMO first wall. *J. Nucl. Mater.*, 438, 2013.

[10] R. Lindau et al. Present development status of EUROFER and ODS-EUROFER for application in blanket concepts. *Fusion Eng Des*, 75-79:989–996, 2005.

[11] C. Dorn et al. A review of physical and mechanical properties of titanium beryllides with specific modern application of TiBe$_{12}$. *Fusion Eng Des*, 84:319–322, 2009.

[12] J.T. Goorley et al. Initial MCNP6 release overview - MCNP6. *version 1.0*, 2013. .

[13] J-Ch Sublet et al. The FISPACT-II user manual. *CCFE-R*, 11(11), 2012.

[14] L.W.G Morgan et al. The development of a fusion specific depletion interface code FATI. *Fusion Eng Des*, 88(11):2891 – 2897, 2013.

[15] R. Forrest et al. FENDL-3 library - Summary document. *INDC(NDS)-628*, 2012.

[16] A.J. Koning et al. Modern nuclear data evaluation with the TALYS code system. *Nuclear Data Sheets*, 113(12):2841 – 2934, 2012. Special Issue on Nuclear Reaction Data.

[17] L. Morgan et al. The impact of time dependant spectra on fusion blanket burn-up. *Fusion Eng Des*, 88:100 – 105, 2013.

[18] N. Taylor et al. A model of the availability of a fusion power plant. *Fusion Eng Des*, 51-52:363–369, 2000.